Copper(III) Complexes of Tripeptides with Histidine and Histamine as the Third Residue

Michael R. McDonald, William M. Scheper, Hsiupu D. Lee, and Dale W. Margerum*

Department of Chemistry, Purdue University, West Lafayette, Indiana 47907

Received May 20, 1994[⊗]

Copper(III) doubly-deprotonated tripeptide complexes of Aib_2His, Ala_2His, Gly_2His, Aib_2Ha, and Gly_2Ha are characterized, where Aib is α-aminoisobutyric acid, Ala is L-alanine, Gly is glycine, His is L-histidine, and Ha is histamine. Reduction potentials (V vs NHE) are evaluated: $Cu^{III}(H_{-2}Aib_2His) = 0.785$, $Cu^{III}(H_{-2}Aib_2Ha)^+ = 0.772$, $Cu^{III}(H_{-2}Gly_2Ha)^+ = 0.925$, $Cu^{III}(H_{-2}Ala_2His) = 0.86$, and $Cu^{III}(H_{-2}Gly_2His) = 0.94$. The pK_a values of 8.2 to 8.7 for amine deprotonation to give the triply-deprotonated copper(III) complexes are 2–3 pK_a units lower for these complexes than for tripeptides that do not contain histidine or histamine. Copper(III)–peptide complexes with histidine as the third residue undergo very rapid oxidative decarboxylation, while the histamine-containing complexes decompose more slowly by proton abstraction of the α hydrogen on the histamine residue. At $p[H^+]$ 7, first-order rate constants for self-decomposition of copper(III) histidine-containing complexes are 10^5 times greater than for those containing histamine. The observed first-order rate constants for the loss of copper(III) for the histidine-containing tripeptides have maximum values at pH 5–7 and decrease at lower pH due to carboxylate protonation and decrease at higher pH due to amine deprotonation. The decomposition of $Cu^{III}(H_{-2}Gly_2Ha)^+$ is general-base assisted with a Brønsted β value of 0.59. As the pH increases, this effect is offset by amine deprotonation. All the peptides are oxidized at the third residue to give the peptide derivative of α-hydroxyhistamine, which dehydrates slowly to give an olefin, the peptide derivative of α,β-dehydrohistamine.

Introduction

Reduction potentials that range from 0.37 to 1.0 V (vs NHE) have been observed for copper(III)–peptide complexes.[1-3] The lower the potential the more stable the complexes; one low potential Cu(III) complex was sufficiently stable to permit the determination of its crystal structure.[4] Although many copper(III)–peptides have been studied,[1-10] little has been reported about copper(III)–peptide complexes with histidine or histamine as the third residue. Structures of the complexes studied in the present work are given in Figure 1. Margerum et al.[1,3] reported that coordination of an imidazole donor in the fourth position of copper(III)–peptide complexes, i.e. those containing histidine or histamine, increases the reduction potential by +0.04 V vs a carboxylate donor and that the 5–5–6 membered ring system of histidine-containing tripeptides increases the reduction potential by +0.02 to +0.04 V. Therefore, reduction potentials are higher for histidine and histamine containing copper(III)–tripeptide complexes relative to other complexes.

Our interest in the copper(III) complexes containing histidine and histamine as the third residue was renewed by the work of Dervan and co-workers.[11] They attached Gly_2His to the amine terminal of a DNA binding agent which, in the presence of

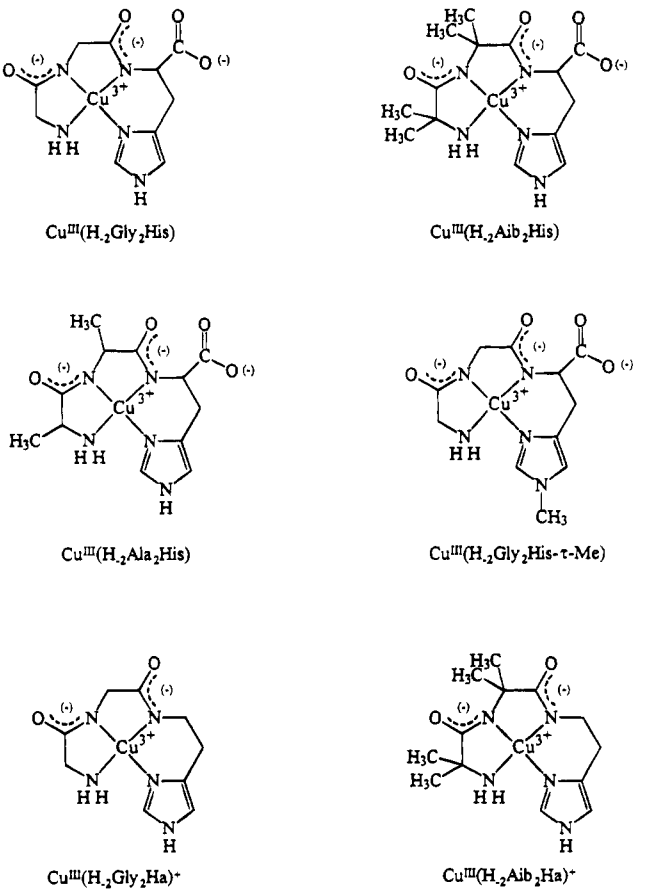

Figure 1. Structures of copper(III) complexes (not all hydrogen atoms are shown).

[⊗] Abstract published in *Advance ACS Abstracts,* December 15, 1994.

(1) Bossu, F. P.; Chellappa, K. L.; Margerum, D. W. *J. Am. Chem. Soc.* **1977**, *99*, 2195–2703.
(2) Anast, J. M.; Hamburg, A. W.; Margerum, D. W. *Inorg. Chem.* **1983**, *22*, 2139–2145.
(3) Margerum, D. W.; Scheper, W. M.; McDonald, M. R.; Fredericks, F. C.; Wang, L.; Lee, H. D. In *Bioinorganic Chemistry of Copper*; Karlin, K. D.; Tyeklar, Z., Eds.; Chapman & Hall: New York, 1993; pp 213–221.
(4) Diaddario, L. L.; Robinson, W. R.; Margerum, D. W. *Inorg. Chem.* **1983**, *22*, 1021–1025.
(5) Owens, G. D.; Margerum, D. W. *Inorg. Chem.* **1981**, *20*, 1446–1453.
(6) Margerum, D. W.; Wang, L.; Scheper, W. M.; Lee, H. D. *J. Inorg. Biochem.* **1991**, *43*, 211.
(7) Margerum, D. W.; Wong, L. F.; Bossu, F. P.; Chellappa, K. L.; Czarnecki, J. J.; Kirksey, S. T.; Neubecker, T. A. In *Bioinorganic Chemistry II*; Raymond, K. N., Ed.; Pergamon Press: Oxford, England, 1977, pp 515–528.
(8) Rybka, J. S.; Kurtz, J. L.; Neubecker, T. A.; Margerum, D. W. *Inorg. Chem.* **1980**, *19*, 2791–2796.
(9) Margerum, D. W. *Pure Appl. Chem.* **1983**, *55*, 23–34.
(10) Hinton, J. P.; Margerum, D. W. *Inorg. Chem.* **1986**, *25*, 3248–3256.
(11) Mack, D. P.; Iverson, B. L.; Dervan, P. B. *J. Am. Chem. Soc.* **1988**, *110*, 7572–7576.

0020-1669/95/1334-0229$09.00/0

copper(II) and oxidizing agents, causes site-specific DNA cleavage. The possibility that copper(III) plays a role in site-specific substrate oxidation prompted this work. Our initial studies have focused on copper(III)−tripeptide complexes with histidine and histamine as the third residue. These complexes are characterized in terms of their oxidizing power, pK_a values for amine deprotonation, rates of self-decomposition, oxidation products, and decomposition mechanisms.

The kinetic stability of copper(III)−peptide complexes decreases with increasing reduction potential and depends on the substituents of the α-carbon of the peptide residues.[3] Replacement of hydrogens at the α-position of the peptide residues with methyl groups increases the stability by decreasing the reduction potential of the complex. We observed such a rapid decarboxylation of the $Cu^{III}(H_{-2}Gly_2His)$ complex that its characterization was difficult. The $Cu^{III}(H_{-2}Aib_2His)$ complex was prepared in order to give a complex with a lower reduction potential that might have a slower rate of decarboxylation, so that the system would be more amenable to study. This assumption proved to be correct and allowed the $Cu^{III}(H_{-2}Aib_2His)$ system to be characterized over a wide pH range. The copper(III) complex of glycylglycylhistamine ($Cu^{III}(H_{-2}Gly_2Ha)^+$), which has no carboxylate group, was prepared in order to compare its reactivity toward self-decomposition to that of $Cu^{III}(H_{-2}Gly_2His)$. Kinetic studies and the products indicate that the rate-determining step for the decomposition of $Cu^{III}(H_{-2}Gly_2Ha)^+$ is proton abstraction from the α-carbon on the histamine residue.

Products of the decomposition of the histidine-containing copper(III) complexes support and provide insight about the pathway leading to the products reported by de Meester and Hodgson[12] and by Sakurai and Nakahara.[13] Our work shows that copper(III) is a probable intermediate in the oxidative decarboxlyation of $Cu^{II}(H_{-2}Gly_2His)^-$ observed by de Meester and Hodgson, where crystals of Cu^{II}(glycylglycyl-α,β-dehydrohistamine) were isolated from a solution that initially contained $Cu^{II}(H_{-2}Gly_2His)^-$ and was exposed to air. We also show that glycylglycyl-α-hydroxyhistamine, which was identified by its NMR spectrum by Sakurai and Nakahara[13] from a solution containing $Ni^{II}(H_{-2}Gly_2His)^-$ and O_2, is a precursor to the formation of glycylglycyl-α,β-dehydrohistamine.

Experimental Section

Reagents. All peptides were synthesized in this laboratory. Solutions were prepared with double-deionized distilled water. A stock solution of $Cu(ClO_4)_2$ was prepared from $CuCO_3$ and $HClO_4$. The solution was standardized by titration with EDTA (Fisher Scientific) with murexide as the indicator. Sodium hexachloroiridate(IV), obtained from Johnson Mathey Inc., was used without further purification. $Ir^{IV}Cl_6^{2-}$ was standardized spectrophotometrically ($\epsilon = 4075\ M^{-1}\ cm^{-1}$ at 490 nm).[5] The ionic strength of all solutions was controlled with analytical reagent grade $NaClO_4$ which was recrystallized from water, redissolved, and standardized gravimetrically.

The copper(II)−peptide complexes were prepared by dissolving the peptide in water and by adding the appropriate amount of standardized $Cu(ClO_4)_2$ so that the peptide was in 5−10% excess. The solution was then adjusted to a pH greater than 6.5 so that the complex would be completely formed.[14]

Methods. An Orion Model 601A digital research pH meter equipped with a Corning combination electrode was used for pH measurements. The electrode was calibrated by titration of standard $HClO_4$ with standard NaOH to correct the measured pH values to $p[H^+]$ values at 25.0 ± 0.1 °C and μ = 1.0 M ($NaClO_4$).

We use $p[H^+] = -\log[H^+]$, because $[H^+]$ values are expressed in molarities rather than in activities ($pH = -\log a_H$). It is essential to use the same units of concentration for all species in the determination of equilibrium constants.

Reduction potentials were determined by Osteryoung square wave voltammetry (OSWV) with a BAS-100 electrochemical analyzer. The average standard deviation was ±4 mV. The working electrode was a glassy carbon electrode (3 mm diameter), the auxiliary electrode was a platinum wire, and the reference electrode was a Vycor tip Ag/AgCl electrode stored in 3 M NaCl (E° = 0.194 V vs NHE). The flow-through bulk electrolysis unit for this work is similar to that reported previously.[15] The column was 0.5 cm (i.d.) × 1.2 cm. The potential was applied with the BAS-100 and maintained at 1.0 V vs Ag/AgCl. The flow-rate was held at 1.0 mL/min with a Gilman Miniplus 2 peristaltic pump. The number of moles of electrons per mole of copper(II)−peptide was determined by measuring the number of coulombs consumed per volume of solution used.

A Varian 5000 HPLC liquid chromatography system equipped with a variable wavelength UV detector and a Whatman Partisil 10 strong cation exchange column (4.6 × 250 mm) was used in product identification. The mobile phase consisted of 0.18 M ammonium formate buffer and 0.20 M NaCl at pH 3.1 in methanol and water (5/95, v/v). A Whatman Magnum 9 strong cation exchange preparative column (9.6 × 250 mm) was used to isolate products for analysis by NMR spectroscopy and mass spectrometry. The mobile phase consisted of 0.18 M ammonium formate in methanol and H_2O (5/95, v/v) at pH 3.1. Fractions of unidentified peaks were collected, freeze-dried, and redissolved in D_2O (99.9%) for analysis by NMR. The wavelength of detection for both analytical and preparative scale separations was 230 nm. NMR spectra were obtained with a Gemini 200 MHz or a Varian VXR 500 MHz spectrometer. Mass spectrometry data were gathered on a Finnigan CI/EI mass spectrometer. Isobutane was used as the carrier gas.

An Orion Model 95-02 carbon dioxide electrode was used to determine the yields of CO_2 from the decomposition of $Cu^{III}(H_{-2}Aib_2His)$. Standards were prepared by adding 5 mL of Orion carbon dioxide buffer solution (95-02-10) to a series of 50 mL standardized carbonate solutions. The final $p[H^+]$ of the solutions was between 4.8 and 5.2. Millivolt measurements were made with an Orion Model 601A digital pH meter. Samples were prepared by flow-through bulk electrolysis of solutions of $Cu^{II}(H_{-2}Aib_2His)^-$ at $p[H^+]$ 13. The $Cu^{III}(H_{-3}Aib_2His)^-$ was immediately neutralized with $HClO_4$ and allowed to decompose. The buffer solution was added and the amount of CO_2 was determined.

UV−vis spectra were measured on a Perkin-Elmer Lambda 9 UV−vis−near-IR spectrometer interfaced to a Zenith 386/20 computer. Kinetic data were obtained with this spectrometer or with a Durrum stopped-flow spectrometer interfaced to a Zenith 151 computer with a MetraByte DASH-16 A/D interface card. Rate constants reported are averages of five trials with standard deviations that ranged from 0.3 to 5.4%. The average percent standard deviation for all rate constants was ± 2%. All kinetic runs were maintained at 25.0 ± 0.1 °C and μ = 1.0 M ($NaClO_4$). Measurements of circular dichroism were obtained with a Jasco Model J600 spectropolarimeter.

Results and Discussion

Formal Reduction Potentials. Electrode potentials (Table 1) for the reversible $Cu^{III/II}(H_{-2}Aib_2His)^{0/-}$, $Cu^{III/II}(H_{-2}Aib_2Ha)^{+/0}$, and $Cu^{III/II}(H_{-2}Gly_2Ha)^{+/0}$ couples are determined from OSWV voltammograms of the copper(II)−peptide complexes in the $p[H^+]$ range 6.5−7.0. These are formal reduction potentials ($E^{\circ\prime}$) based on concentrations rather than activities, and the values in parentheses represent one standard deviation of the error in the last digit of the adjacent number. Amine deprotonation and decomposition rates of these copper(III)−peptide complexes do not interfere with voltammetry measurements in this $p[H^+]$ range.

(12) de Meester, P.; Hodgson, D. *J. Am. Chem. Soc.* **1976**, *98*, 7086−7087.
(13) Sakurai, I.; Nakahara, A. *Inorg. Chim. Acta* **1979**, *34*, L243−L244.
(14) Hay, R. W.; Hassan, M. M.; You-Quan, C. *J. Inorg. Biochem.* **1993**, *52*, 17−25.
(15) Neubecker, T. A.; Kirksey, S. T., Jr.; Chellappa, K. L.; Margerum, D. W. *Inorg. Chem.* **1979**, *18*, 444−448.

Scheme 1. Carboxylate Protonation and Amine Deprotonation for Cu(III) Tripeptides

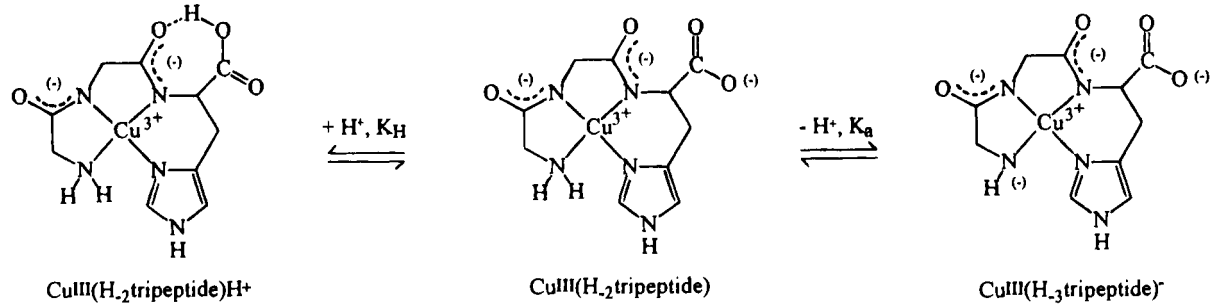

$Cu^{III}(H_{-2}tripeptide)H^+$ $Cu^{III}(H_{-2}tripeptide)$ $Cu^{III}(H_{-3}tripeptide)^-$

Table 1. Formal Reduction Potentials and Amine Deprotonation pK_a values for Copper(III) Complexes[a]

complex	$E^{\circ\prime}$, V	pK_a
$Cu^{III}(H_{-2}Gly_2His)$	0.94[b]	8.2(1)[c]
$Cu^{III}(H_{-2}Gly_2Ha)^+$	0.925(4)	8.37(1)[d]
$Cu^{III}(H_{-2}Ala_2His)$	0.86[b]	8.2(1)[c]
$Cu^{III}(H_{-2}Aib_2His)$	0.785(4)	8.66(4)[d]
$Cu^{III}(H_{-2}Aib_2Ha)^+$	0.772(4)	8.70(5)[d]

[a] 25.0 °C, μ = 1.0 M ($NaClO_4$), $E^{\circ\prime}$ vs NHE. [b] Evaluated from other $E^{\circ\prime}$ measurements. [c] Determined from kinetic data. [d] Determined from voltammetry data.

On the other hand, determination of the $E^{\circ\prime}$ values for the $Cu^{III/II}(H_{-2}Ala_2His)^{0/-}$ and $Cu^{III/II}(H_{-2}Gly_2His)^{0/-}$ couples are complicated because of the extremely rapid decomposition of their copper(III) complexes. This decomposition gives copper(II) complexes of oxidized peptide products that are reoxidized in the voltammetric wave. Therefore, the observed potentials for the Ala_2His and Gly_2His complexes are actually from a mixture of copper–peptide complexes. Faster voltage scans cannot be used with peptide complexes because of limitations due to the heterogeneous kinetic response of the electrode. As a result these potentials could not be measured directly. Previous reports[1,3,6] that gave a reduction potential of 0.98 V for $Cu^{III/II}(H_{-2}Gly_2His)^{0/-}$ were in error because of rapid Cu(III) decomposition reactions. We now propose that 0.94 V is a more accurate $E^{\circ\prime}$ value for the Gly_2His complex, where $E^{\circ\prime}_{Gly_2His} = E^{\circ\prime}_{Gly_2Ha} + (E^{\circ\prime}_{Aib_2His} - E^{\circ\prime}_{Aib_2Ha})$. This is based on the assumption that the difference in $E^{\circ\prime}$ between Gly_2His and Gly_2Ha will be the same as the difference in $E^{\circ\prime}$ between Aib_2His and Aib_2Ha. The $E^{\circ\prime}$ of 0.86 V for the Ala_2His complex was evaluated from $E^{\circ\prime}_{Aib_2His} + {}^1/_2(E^{\circ\prime}_{Gly_2His} - E^{\circ\prime}_{Aib_2His})$. This is based on a total of two methyl substituents in Ala_2 compared to zero and four methyl substituents for Gly_2 and Aib_2, respectively. These predictions are in agreement with the ~0.04 V decrease in reduction potential which occurs per methyl group substituted at the α-position of the peptide.[1]

pK_a of Amine Deprotonation. Doubly-deprotonated copper(III)–tripeptide complexes can deprotonate at the terminal amine bound to copper(III) to form the triply-deprotonated complex, $Cu^{III}(H_{-3}tripeptide)$, as shown in Scheme 1. Amine deprotonation was observed for tripeptides in this study by a decrease in reduction potential, a decrease in reactivity towards self-decomposition, and spectral shifts of their UV–vis absorption bands. The K_a values for amine deprotonation for $Cu^{III}(H_{-2}Aib_2His)$, $Cu^{III}(H_{-2}Aib_2Ha)^+$, and $Cu^{III}(H_{-2}Gly_2Ha)^+$ were determined by measuring their electrode potentials as a function of $p[H^+]$. The copper(II)–peptide complexes do not undergo amine deprotonation, so the reduction potentials decrease as the pH increases. A decrease in reduction potential due to amine deprotonation for copper(III)–peptide complexes of Gly_3a, Gly_4, Gly_5, and Gly_6 has been reported previously.[7,15] Equations 1 and 2 represent the reduction and deprotonation reactions, respectively, for the Aib_2His system. The reduction potential

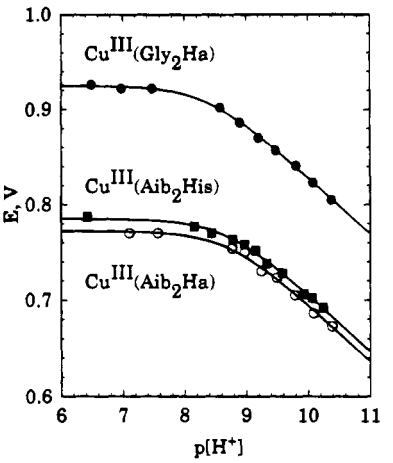

Figure 2. Dependence of the reduction potential (E vs NHE) on $p[H^+]$ for $Cu^{III}(H_{-2}Aib_2His)$, $Cu^{III}(H_{-2}Aib_2Ha)^+$, and $Cu^{III}(H_{-2}Gly_2Ha)^+$, at 25.0 ± 0.1 °C, μ = 1.0 M ($NaClO_4$). Data are fit to eq 4.

$$Cu^{III}(H_{-2}Aib_2His) + e^- \rightleftharpoons Cu^{II}(H_{-2}Aib_2His)^- \quad (1)$$

$$Cu^{III}(H_{-2}Aib_2His) \overset{K_a}{\rightleftharpoons} Cu^{III}(H_{-3}Aib_2His)^- + H^+ \quad (2)$$

is given by eq 3 and can be written in terms of K_a and $[H^+]$ (eq 4). Values for $E^{\circ\prime}$ and K_a were determined from a nonlinear

$$E = E^{\circ\prime} - \frac{RT}{nF}\ln\left(\frac{[Cu^{II}(H_{-2}Aib_2His)^-]}{[Cu^{III}(H_{-2}Aib_2His)]}\right) \quad (3)$$

$$E = E^{\circ\prime} - \frac{RT}{nF}\ln\left(\frac{K_a + [H^+]}{[H^+]}\right) \quad (4)$$

least-squares fit of the data (E vs $[H^+]$) to eq 4 as shown in Figure 2 for all three systems. The values determined for the pK_a for amine deprotonation at 25.0 ± 0.1 °C and μ = 1.0 M ($NaClO_4$) are given in Table 1. The $E^{\circ\prime}$ values determined from the fit of the data to eq 4 are in agreement with the values determined in the $p[H^+]$ range of 6.5–7.0. The pK_a values for $Cu^{III}(H_{-2}Gly_2His)$ and $Cu^{III}(H_{-2}Ala_2His)$ were determined from kinetic measurements that are discussed later.

The UV–vis spectra of $Cu^{III}(H_{-3}Aib_2His)^-$ and $Cu^{III}(H_{-2}Aib_2His)H^+$ are shown in Figure 3. The $Cu^{III}(H_{-3}Aib_2His)^-$ species was generated at $p[H^+]$ 13 by flow-through bulk electrolysis. Acidification of this solution gave the $Cu^{III}(H_{-2}Aib_2His)H^+$ species. The spectra were recorded within 1–2 min after preparation. The rapid loss of copper(III) interfered with the determination of the molar absorptivity of these species. In acid the spectrum of $Cu^{III}(H_{-2}Aib_2His)H^+$ has peaks at 272 and 400 nm, consistent with spectra reported for other copper(III)–peptide complexes.[15] In base, amine deprotonation to form $Cu^{III}(H_{-3}Aib_2His)^-$ shifts the spectrum to give a broad

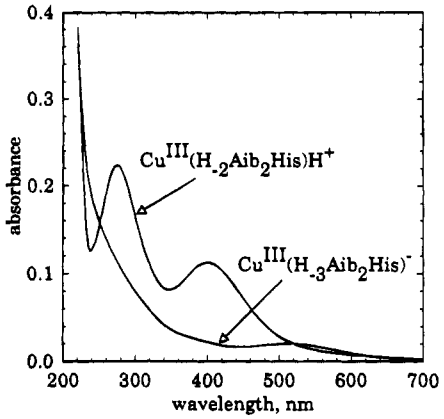

Figure 3. UV−vis spectra of $Cu^{III}(H_{-2}Aib_2His)H^+$ (p[H^+] = 0.6) and $Cu^{III}(H_{-3}Aib_2His)^-$ (p[H^+] = 13.0). Path length = 0.1 cm, μ = 1.0 M $NaClO_4$, and $[Cu^{III}peptide]_{initial} = 5 \times 10^{-4}$ M.

peak centered at 513 nm. Similar spectral shifts have been observed for other amine-deprotonation reactions of copper(III)−peptides.[9,10]

Voltammetry studies of $Cu^{III}(H_{-2}Gly_2His)$ and $Cu^{III}(H_{-2}Gly_2His$-τ-Me) have shown that deprotonation occurs at the amine nitrogen and not at the pyrrole nitrogen in the imidazole ring.[3] The copper(III) histidine and histamine-containing complexes in this study are 5−5−6 ring chelate systems with pK_a values between 8.2 and 8.7. The pK_a values for amine deprotonation of copper(III)−peptides with 5−5−5 and 5−5−6 membered ring systems without histidine or histamine are 2−3 units higher.[16] The lower pK_a values for histidine and histamine-containing tripeptides must be due in part to the ability of the imidazole group to accept electron density through π-back-bonding. Other copper(III)−peptide complexes have a carboxylate group, a deprotonated peptide nitrogen, or a deprotonated amide in the fourth position. None of these groups has the ability to accept electron density resulting from amine deprotonation as well as the imidazole group.

Preparation of Copper(III)−Peptide Complexes. In past work, many copper(III)−peptide complexes were prepared by oxidation of copper(II)−peptide complexes in a flow-through bulk electrolysis column.[15] This method of preparation is possible with the more kinetically stable copper(III) complexes. The $Cu^{III}(H_{-2}Aib_2Ha)^+$ and $Cu^{III}(H_{-2}Gly_2Ha)^+$ complexes are sufficiently stable to be prepared in this way at p[H^+] 6.5−7.5, but the histidine complexes decompose too rapidly. However, the amine-deprotonated complex, $Cu^{III}(H_{-3}Aib_2His)^-$, could be generated in 0.1 M NaOH. Immediately after preparation this solution was mixed with $HClO_4$ solutions to permit decomposition of the copper(III) complex to be observed between p[H^+] 12 and 13 and also between p[H^+] 0 and 2.5. The solution temperature was preadjusted to compensate for the heat of neutralization of the acid and base. For less extreme p[H^+] conditions the Cu(III) complex of Aib_2His was generated by chemical oxidation.

Attempts to prepare the histidine-containing copper(III)−peptide complexes by flow-through bulk electrolysis of copper(II)−peptide solutions in the p[H^+] range 6.5−7.0 were unsuccessful. More than two moles of electrons were released per mole of copper(II)−peptide passing through the electrolysis column because these copper(III)−peptide complexes decompose so rapidly that their copper(II)−peptide products were reoxidized within the column. Therefore, bulk electrolysis of the histidine-containing complexes produced copper(III) complexes of the decomposition products rather than of the original peptide.

Earlier results[3] for the bulk electrolysis of $Cu^{II}(H_{-2}Gly_2His)^-$ reported the complete loss of Gly_2His and 100% yield of CO_2 when 2 equiv or more of electrons are released per Cu^{II}. This is consistent with repeated cycles of oxidation while the solutions are still in the bulk electrolysis column. Each one electron oxidation cycle causes a 50% loss of Gly_2His.

The rapid decomposition of the copper(III) histidine-containing peptides required their preparation in situ by oxidation with $Ir^{IV}Cl_6^{2-}$ (eq 5). This method of preparation allowed the

$$Cu^{II}peptide + Ir^{IV}Cl_6^{2-} \underset{k_{-1}}{\overset{k_1}{\rightleftharpoons}} Cu^{III}peptide + Ir^{III}Cl_6^{3-} \quad (5)$$

decomposition reaction of the copper(III)−peptide complexes shown in eq 6 to be studied as a function of pH. The values of

$$2Cu^{III}peptide \xrightarrow{k_{obsd}} Cu^{II}products + Cu^{II}peptide + CO_2 \quad (6)$$

the equilibrium constant, K, for eq 5 were determined from the copper(III) reduction potentials given in Table 1 and the reduction potential of $IrCl_6^{2-}$ (0.892 V vs NHE).[1] The concentrations of the copper(II)−peptides were 10−200-fold greater than the $IrCl_6^{2-}$ concentration to ensure that the reaction in eq 5 would go to at least 97% completion. The consumption of all of the $IrCl_6^{2-}$ also prevents oxidation of copper(II) products that are formed in eq 6.

The rate of electron transfer for the formation of the copper(III)−peptide complexes (k_1 in eq 5) can be predicted based on work by Owens and Margerum.[5] The values of K, $[Cu^{II}peptide]_{init}$, $[Ir^{IV}Cl_6^{2-}]_{init}$, the percent copper(III)−peptide formed (based on the Ir(IV) reacted), the predicted pseudo-first-order rate constant (k_f) for the formation of the copper(III)−peptide complex, and the observed rate constant for the loss of copper(III)−peptide (k_{obsd}) are given in Table 2. The observed rate constants for the loss of copper(III) were 2−4 orders of magnitude smaller than the predicted pseudo-first-order electron transfer rate constants. Therefore, decomposition of the copper(III)−peptide complex (eq 6) is not limited by the electron transfer step (eq 5).

Table 2. Formation of Copper(III)−Peptide Complexes by Chemical Oxidation with $Ir^{IV}Cl_6^{2-}$ [a]

	Aib_2His	Ala_2His	Gly_2His
$[Cu^{II}peptide]_{init}$, M	2.65×10^{-4}	4.71×10^{-3}	6.60×10^{-3}
$[Ir^{IV}Cl_6^{2-}]_{init}$, M	2.15×10^{-5}	3.09×10^{-5}	3.23×10^{-5}
K [b]	64.4	2.86	0.154
% yield of Cu(III) [c]	99.8	99.8	97.0
formation rate constant, k_f, s^{-1} [d]	3.5×10^4	6.6×10^4	2.0×10^4
range decomp. constants, k_{obsd}, s^{-1} [e]	0.019−3.17	0.48−20.3	0.80−128

[a] 25.0 °C, μ = 1.0 M ($NaClO_4$). [b] $K = ([Cu^{III}peptide][Ir^{III}Cl_6^{3-}])/([Cu^{II}peptide][Ir^{IV}Cl_6^{2-}])$. [c] Calculated value based on $[Ir^{IV}Cl_6^{2-}]_{init}$. [d] $k_f = k_1[Cu^{II}peptide]$, based on k_1 values predicted from ref 5. [e] Rate constants for the loss of Cu^{III}peptide with p[H^+] variation.

Decomposition Kinetics of $Cu^{III}(H_{-2}Gly_2His)$, $Cu^{III}(H_{-2}Ala_2His)$, and $Cu^{III}(H_{-2}Aib_2His)$. $Cu^{III}(H_{-2}Gly_2His)$ and $Cu^{III}(H_{-2}Ala_2His)$ were generated within a stopped-flow cell by chemical oxidation with $Ir^{IV}Cl_6^{2-}$ (eq 5) in the p[H^+] range of 7.0−10.4. The loss of copper(III)−peptide (monitored at 400 nm) was first order in Cu(III) and the rate constants decreased as the p[H^+] increased (Figure 4). The mechanisms for the decomposition of $Cu^{III}(H_{-2}Gly_2His)$ and $Cu^{III}(H_{-2}Ala_2His)$, in the p[H^+] range studied, are similar. Both undergo oxidative

(16) Fredericks, F. C. M.S. Thesis, Purdue University, West Lafayette, IN, 1993, p 33.

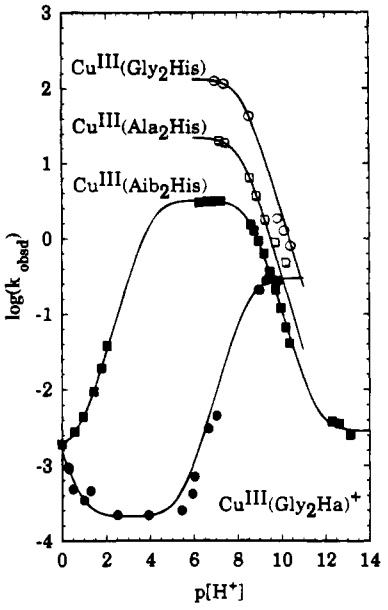

Figure 4. Decomposition rate constants vs p[H$^+$] for $Cu^{III}(H_{-2}Aib_2His)$, $Cu^{III}(H_{-2}Ala_2His)$, $Cu^{III}(H_{-2}Gly_2His)$, and $Cu^{III}(H_{-2}Gly_2Ha)^+$, at 25.0 ± 0.1 °C, μ = 1.0 M ($NaClO_4$).

decarboxylation with loss of copper(III). The mechanism involves amine deprotonation and a self-decomposition path as summarized for $Cu^{III}(H_{-2}Gly_2His)$ in eqs 7–9. The rate

$$Cu^{III}(H_{-2}Gly_2His) \overset{K_a}{\rightleftharpoons} Cu^{III}(H_{-3}Gly_2His)^- + H^+ \quad (7)$$

$$Cu^{III}(H_{-2}Gly_2His) \xrightarrow{k_d} \text{intermediate} + CO_2 \quad (8)$$

$$Cu^{III}(H_{-2}Gly_2His) + \text{intermediate} \xrightarrow{\text{fast}} \text{products} \quad (9)$$

$$\frac{-d[Cu^{III}(Gly_2His)]_{tot}}{dt} = k_{obsd}[Cu^{III}(Gly_2His)]_{tot} \quad (10)$$

$$k_{obsd} = \frac{2k_d}{1 + K_a/[H^+]} \quad (11)$$

expression is given in eq 10, where $[Cu^{III}(Gly_2His)]_{tot} = [Cu^{III}(H_{-2}Gly_2His)] + [Cu^{III}(H_{-3}Gly_2His)^-]$. A second Cu(III) reacts rapidly with the intermediate to give stable two-electron peptide oxidation products (eq 9). This accounts for the factor of 2 in the expression for k_{obsd} in eq 11. The data and the fit of the data to eq 11 are shown in Figure 4 for both the $Cu^{III}(H_{-2}Gly_2His)$ and $Cu^{III}(H_{-2}Ala_2His)$ systems. The values of k_d and pK_a determined from the fit of the data are listed in Table 3.

The increase in stability of the $Cu^{III}(H_{-2}Aib_2His)$ complex made it possible to study its decomposition kinetics over the p[H$^+$] range 0–13. All reaction traces were first-order in the loss of Cu(III) monitored at 420 nm. The observed first-order rate constants are very pH dependent as shown in Figure 4. This dependence is due to rapid acid/base reactions that involve carboxylate protonation and amine deprotonation of $Cu^{III}(H_{-2}Aib_2His)$. There are 3 forms of this tripeptide complex, as shown in Scheme 1. In the p[H$^+$] range 7–10 the mechanism is similar to that of $Cu^{III}(H_{-2}Gly_2His)$ and $Cu^{III}(H_{-2}Ala_2His)$. A mechanism that describes the behavior over the entire pH range is shown in Scheme 2, where the rate-determining step is decarboxylation. At low p[H$^+$] values protonation of the carboxylate group gives $Cu^{III}(H_{-2}Aib_2His)H^+$. This type of protonation of donor groups outside those in the first coordination sphere has been observed previously for other peptide complexes.[8,17,18]

Protonation of a metal–peptide carboxylate group that can hydrogen bond to a peptide oxygen (as depicted in Scheme 1) occurs with protonation equilibrium constants (M^{-1} at 25.0 °C) of $10^{4.1}$ (μ = 0.10 M)[17] for $[Ni^{II}(H_{-3}Gly_4)H]^-$, $10^{4.2}$ (μ = 1.0 M)[18] for $Cu^{II}(H_{-2}Gly_2His)H$, and $10^{4.3}$ (μ = 1.0 M)[8] for $Cu^{III}(H_{-3}Gly_4)H$. Our observed kinetic dependence fits an outside protonation constant of $10^{4.05}$ (μ = 1.0 M) for $Cu^{III}(H_{-2}Aib_2His)H^+$. Carboxylate protonation blocks the decarboxylation step and thereby stabilizes the copper(III)–peptide. In neutral solutions, $Cu^{III}(H_{-2}Aib_2His)$ is the predominant species. Amine deprotonation occurs at high p[H$^+$] to give $Cu^{III}(H_{-3}Aib_2His)^-$, which is considerably more stable than $Cu^{III}(H_{-2}Aib_2His)$ due to its lower reduction potential. Figure 4 shows an unusual arch-shaped curve for the dependence of log k_{obsd} (k_{obsd} is defined experimentally in eqs 12 and 13) on

$$\frac{-d[Cu^{III}(Aib_2His)]_{tot}}{dt} = k_{obsd}[Cu^{III}(Aib_2His)]_{tot} \quad (12)$$

$$[Cu^{III}(Aib_2His)]_{tot} = [Cu^{III}(H_{-2}Aib_2His)H^+] + [Cu^{III}(H_{-2}Aib_2His)] + [Cu^{III}(H_{-3}Aib_2His)^-] \quad (13)$$

p[H$^+$]. The dependence of k_{obsd} from p[H$^+$] 1 to 11 can be accounted for in terms of $Cu^{III}(H_{-2}Aib_2His)$ as the only reactive species. Inhibition occurs due to carboxylate protonation below p[H$^+$] 5 and due to amine deprotonation above p[H$^+$] 7, as shown in Scheme 2. Below pH 1 the degree of acid inhibition lessens, so we have assigned a H$^+$-assisted rate constant, k_H, for the decomposition of $Cu^{III}(H_{-2}Aib_2His)$. Above p[H$^+$] 11, the base inhibition lessens, so we have assigned a OH$^-$-assisted rate constant, k_{OH}, as shown in Scheme 2. Although these acid and base paths cannot be distinguished kinetically from direct decomposition reactions of the $Cu^{III}(H_{-2}Aib_2His)H^+$ and $Cu^{III}(H_{-3}Aib_2His)^-$ species, we prefer the paths assigned in Scheme 2. This mechanism results in a k_{obsd} dependence on acid and base concentrations as given in eq 14. The factor of

$$k_{obsd} = \frac{2(k_d + k_H[H^+] + k_{OH}[OH^-])}{1 + K_H[H^+] + K_a[OH^-]/K_w} \quad (14)$$

2 in eq 14 is a result of the oxidation of the proposed $Cu^{I}(H_{-1}Aib_2DHP)$ complex (DHP designates a dehydropeptide with a N=C group) by $Cu^{III}(H_{-2}Aib_2His)$ as shown in Scheme 2. A 50% recovery of $Cu^{II}(H_{-2}Aib_2His)^-$ is predicted by this mechanism, and this was confirmed experimentally. Equilibrium and rate constants in eq 14 were determined to give the fit of the data shown in Figure 4. The values of k_d, k_H, k_{OH}, pK_a, and pK_H, where pK_w = 13.60,[19] are listed in Table 3. The value of 8.55 ± 0.03 for the pK_a of amine deprotonation determined from these kinetic measurements is consistent with the value of 8.66 ± 0.04 determined by voltammetry.

In an earlier report,[3] we speculated that an unusual rearrangement might occur during decarboxylation that would lead to copper–carbon bond formation at the α-carbon atom of histidine. At that time, our preliminary kinetic results indicated

(17) Paniago, E. B.; Margerum, D. W. *J. Am. Chem. Soc.* **1972**, *94*, 6704–6710.
(18) Wong, L. F.; Cooper, J. C.; Margerum, D. W. *J. Am. Chem. Soc.* **1976**, *98*, 7268–7274.
(19) Molina, M.; Melios, C.; Tognolli, J. O.; Luchiari, L. C.; Jafelicci, M., Jr. *J. Electroanal. Chem. Interfacial Electrochem.* **1979**, *105*, 237–246.

Table 3. Rate and Equilibrium Constants for Cu(III)–Histidine and Cu(III)–Histamine Tripeptide Complexes[a]

	complex			
constant	$Cu^{III}(H_{-2}Aib_2His)$	$Cu^{III}(H_{-2}Ala_2His)$	$Cu^{III}(H_{-2}Gly_2His)$	$Cu^{III}(H_{-2}Gly_2Ha)^+$
k_d, s^{-1}	1.62(8)	11.3(2)	67.9(9)	$1.0(3) \times 10^{-4}$
k_H, $M^{-1}\ s^{-1}$	8.3(6)			$7(2) \times 10^{-4}$
k_{OH}, $M^{-1}\ s^{-1}$	$1.8(2) \times 10^2$			$2.0(5) \times 10^4$
pK_a[b]	8.55(0.03)[c]	8.2(0.1)[c]	8.2(0.1)[c]	8.5(0.1)[c]
	8.66(0.04)[d]			8.37(0.04)[d]
log K_H[e]	4.05(0.02)[c]			

[a] Conditions: 25.0 °C, μ = 1.0 M ($NaClO_4$). [b] Amine deprotonation. [c] Determined from kinetic fit vs p[H^+]. [d] Determined from voltammetric fit vs p[H^+]. [e] Carboxylate protonation.

Scheme 2. Reaction Mechanism for the Decomposition of $Cu^{III}(H_{-2}Aib_2His)$

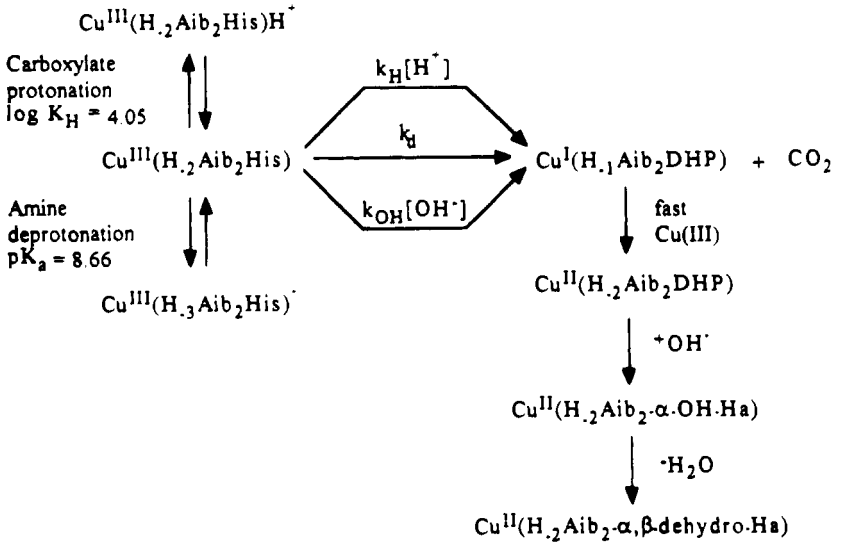

that the decarboxylation rate increased greatly as the acidity of the solution increased from pH 7.5 to 6.5. The complete pH dependence in the present work (Figure 4) shows that this is not the case. The k_{obsd} values for the decomposition of the Cu(III) peptides (with histidine in the third residue) level off between pH 7.5 and 5 and decrease below pH 5. We believe that these results are inconsistent with a rearrangement in which a proton must be added to the peptide nitrogen. Furthermore, we are unable to observe a slow second step in which the intermediate rearranges again to give the α-hydroxy product and reforms the copper–N(peptide) bond. Therefore, we postulate that the intermediate in eqs 8 and 9 is either a Cu^I–dehydropeptide or is a Cu^{II}–carbon radical rather than a copper–carbon-bonded species. Either of these intermediates will react rapidly with a second Cu(III) peptide.

The study of the decomposition of $Cu^{III}(H_{-2}Aib_2His)$, $Cu^{III}(H_{-2}Ala_2His)$, and $Cu^{III}(H_{-2}Gly_2His)$ enabled the rate of decomposition for the histidine-containing tripeptides to be compared as a function of reduction potentials that span 155 mV. There is a linear relationship between the log k_d and the reduction potential as shown in Figure 5. The sensitivity of the rate of decomposition to the value of the reduction potential for these decarboxylation reactions is similar to those found where the rate-determining step is not decarboxylation.[3]

Decomposition Kinetics of $Cu^{III}(H_{-2}Gly_2Ha)^+$. $Cu^{III}(H_{-2}Gly_2Ha)^+$ was prepared by electrochemical methods discussed previously. Precautions were taken to avoid multiple oxidations in the bulk electrolysis procedure. Absorbance vs time traces for the loss of copper(III), observed at 400 nm, were first-order from p[H^+] 0.3 to 9.9. The k_{obsd} values are given in terms of $Cu^{III}(Gly_2Ha)_{tot}$ with definitions similar to eqs 12 and 13, except that in the absence of a carboxylate group there is no appreciable outside protonation.

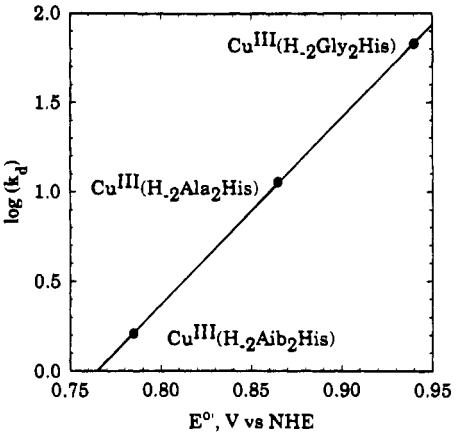

Figure 5. Dependence of the self-decomposition rate constants (k_d) for histidine containing tripeptides on the reduction potentials of the Cu(III) complexes.

The mechanism for the decomposition of $Cu^{III}(H_{-2}Gly_2Ha)^+$ involves amine deprotonation (eq 15), a self-decomposition path

$$Cu^{III}(H_{-2}Gly_2Ha)^+ \rightleftharpoons Cu^{III}(H_{-3}Gly_2Ha) + H^+,\ K_a \quad (15)$$

$$Cu^{III}(H_{-2}Gly_2Ha)^+ \xrightarrow{k_d} \text{intermediate} \quad (16)$$

$$Cu^{III}(H_{-2}Gly_2Ha)^+ + H^+ \xrightarrow{k_H} \text{intermediate} \quad (17)$$

$$Cu^{III}(H_{-2}Gly_2Ha)^+ + OH^- \xrightarrow{k_{OH}} \text{intermediate} \quad (18)$$

(eq 16), an acid path (eq 17), and a base path (eq 18). In the

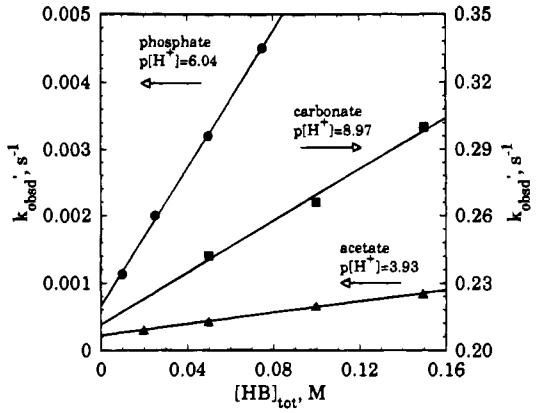

Figure 6. Dependence of the observed first-order rate constant for the decomposition of $Cu^{III}(H_{-2}Gly_2Ha)^+$ as a function of acetate, phosphate, and carbonate concentrations.

presence of acetate, phosphate, and carbonate buffers a dependence on the concentration of the basic form of the buffer (eq 19) was also observed. We define k_{obsd}' as the first-order rate

$$Cu^{III}(H_{-2}Gly_2Ha)^+ + B^- \xrightarrow{k_B} \text{intermediate} + HB \quad (19)$$

constant in the presence of buffer and k_{obsd} as the constant in the absence of buffers. The mechanism leads to eqs 20 and 21. The buffer dependence is shown in eq 22 and Figure 6,

$$k'_{obsd} = \frac{2(k_d + k_H[H^+] + k_{OH}[OH^-] + k_B[B^-])[H^+]}{[H^+] + K_a} \quad (20)$$

$$k_{obsd} = \frac{2(k_d + k_H[H^+] + k_{OH}[OH^-])[H^+]}{[H^+] + K_a} \quad (21)$$

$$k'_{obsd} = k_{obsd} + \left(\frac{2k_B[H^+]}{[H^+] + K_a}\right)\left(\frac{K_a^{HB}[HB]_{tot}}{K_a^{HB} + [H^+]}\right) \quad (22)$$

where $[HB]_{tot} = [B^-] + [HB]$ and $K_a^{HB} = [H^+][B^-]/[HB]$. Values of k_B for acetate, phosphate, and carbonate are used to correct the k'_{obsd} rate constant in order to evaluate k_{obsd} for the pH dependence plot of $Cu^{III}(Gly_2Ha)$ shown in Figure 4. The resolved constants are $k_d = (1.0 \pm 0.3) \times 10^{-4}$ s^{-1}, $k_H = (7 \pm 2) \times 10^{-4}$ M^{-1} s^{-1}, $k_{OH} = (2.0 \pm 0.5) \times 10^4$ M^{-1} s^{-1} and $pK_a = 8.5 \pm 0.1$ (amine deprotonation). The latter value is in good agreement with the pK_a value of 8.37 ± 0.04 determined from voltammetric data. The k_d value is a factor of 6.8×10^5 smaller than for $Cu^{III}(H_{-2}Gly_2His)$, which illustrates the importance of the rapid decarboxylation path for the histidine peptide.

The buffer dependence is a result of general-base catalysis by B^- in the abstraction of a proton in the rate-determining step. The rate constants (k_B) show a Brønsted relationship (eq 23),[20] where p is the number of equivalent proton sites on HB,

$$\log\left(\frac{k_B}{q}\right) = \log(G_B) + \beta \log\left(\frac{p}{qK_a^{HB}}\right) \quad (23)$$

q is the number of equivalent basic sites on B^-, G_B is the proportionality constant, and β is the Brønsted coefficient. The β value can range from 0 to 1 and reflects the degree of proton transfer in the transition state. A large β value represents a large degree of proton transfer in the transition state of the rate determining step. Table 4 summarizes the values of p, q, k_B, and K_a^{HB} for each buffer including H_2O and OH^-. Figure 7 is a Brønsted plot with a slope (β) of 0.59 ± 0.02. Rate constants for the base-catalyzed decomposition increase with increasing base strength as predicted by the Brønsted relationship. This correlation shows that proton abstraction is the rate-determining step in this copper(III) decomposition.

(20) Bell, R. P. *The Proton in Chemistry*, 2nd ed.; Cornell University: Ithaca, NY, 1973; p 198.

Table 4. Summary of Constants for Brønsted Relationship[a]

B	p[b]	q[c]	pK_a^{HB}	k_B, M^{-1} s^{-1}
H_2O	3	2	−1.74[d]	$1.8(3) \times 10^{-6}$ [e]
CH_3COO^-	1	2	4.55[f]	0.0109(3)
HPO_4^{2-}	2	3	6.46[g]	0.094(2)
CO_3^{2-}	1	3	9.57[h]	7.2(7)
OH^-	2	3	15.39[i]	$2.0(5) \times 10^4$

[a] Conditions: 25.0 °C, μ = 1.0. [b] p is the number of equivalent proton sites on HB. [c] q is the number of equivalent basic sites on B^-. [d] −log(55.5). [e] $k_B = k_d/55.5$. [f] Barcza, L.; Mihályi, K. F. *Phys. Chem.* **1977**, *104*, 199−212. [g] Smith, R. S.; Martell, A. E. *Critical Stability Constants*; Plenum: New York, 1976; Vol. 4, p 56. [h] *Ibid.* p 37. [i] K_w/55.5, M.

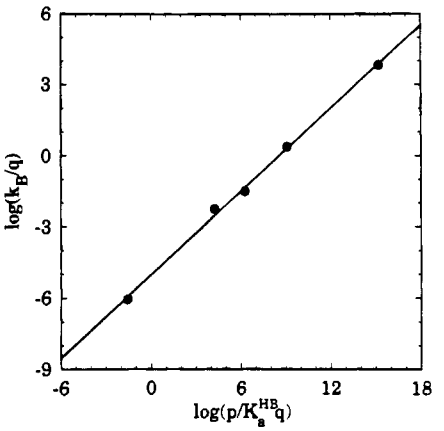

Figure 7. Brønsted plot for the reaction of $Cu^{III}(H_{-2}Gly_2Ha)^+ + B^-$, where k_B is the second-order rate constant and K_a^{HB} is the ionization constant of HB. Slope (β) = 0.59 ± 0.02.

Decomposition Products of $Cu^{III}(H_{-2}Aib_2His)$ and $Cu^{III}(H_{-2}Gly_2His)$. Decarboxylation of $Cu^{III}(H_{-2}Aib_2His)$ and $Cu^{III}(H_{-2}Gly_2His)$ was confirmed by the formation of CO_2 and the loss of the chiral center in the histidine residue. The amount of CO_2 produced from the decomposition of $Cu^{III}(H_{-2}Aib_2His)$ was determined with a carbon dioxide electrode to be 45 ± 15% (at $p[H^+] = 5.0$) relative to the initial concentration of $Cu^{III}(H_{-2}Aib_2His)$, assuming complete oxidation during flow-through bulk electrolysis. This result is consistent with the mechanism proposed in Scheme 2, where only 50% of $Cu^{III}(H_{-2}Aib_2His)$ decarboxylates. Carbon dioxide was also observed as a decomposition product of $Cu^{III}(H_{-2}Gly_2His)$.[3] A decrease in optical activity was observed for copper(II) decomposition products relative to initial concentrations of $Cu^{II}(H_{-2}Gly_2His)^-$ and $Cu^{II}(H_{-2}Aib_2His)^-$ before oxidation, which indicates loss of the original peptide. The circular dichroic data for the Aib_2His system, Table 5, show that in the $p[H^+]$ range 2.0−9.3 that ~ 50% of the Aib_2His is recovered and at $p[H^+]$ 12.65 that ~77% is recovered.

Four products were observed by HPLC after the decomposition of $Cu^{III}(H_{-2}Aib_2His)$. Copper(II) and Aib_2His were identified as two of the products from HPLC standards. The percent recovery of Aib_2His, listed in Table 5, was determined as a function of $p[H^+]$ by HPLC. In the $p[H^+]$ range 1.6−9.9 the percent recovery of Aib_2His is ~ 50%. At $p[H^+]$ 12.65 the percent recovery of Aib_2His is 64−72%. The HPLC and circular dichroism data are in agreement. Higher yields of Aib_2-

Table 5. Recovery of Aib_2His from the Decomposition of $Cu^{III}(H_{-2}Aib_2His)$ Determined by Liquid Chromatography and Circular Dichroism[a]

p[H+]	% Aib_2His recovered	method
1.58	50 ± 1	HPLC
2.00	45 ± 2	CD
4.64	51 ± 5	HPLC
6.34	43 ± 2	CD
6.69	46 ± 1	HPLC
9.32	55 ± 2	CD
9.92	50 ± 2	HPLC
12.65	64 ± 2	HPLC
12.65	72 ± 1	HPLC
12.65	77 ± 2	CD

[a] HPLC detection at 230 nm; CD scan from 300−500 nm.

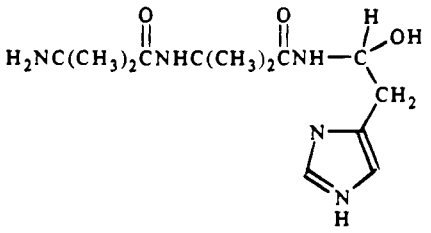

α-aminoisobutyryl-α-aminoisobutyryl-α-hydroxyhistamine
(Aib_2-α-OH-Ha)

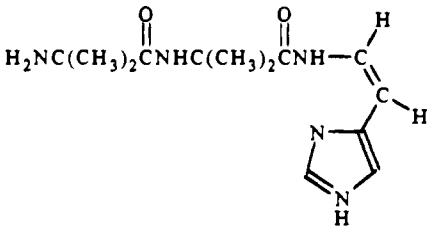

α-aminoisobutyryl-α-aminoisobutyryl-α,β-dehydrohistamine
(Aib_2-α,β-dehydro-Ha)

Figure 8. Oxidized products of Aib_2His.

His determined by HPLC and circular dichroism at p[H+] 12.65 indicate that decomposition products undergo further oxidation by $Cu^{III}(H_{-2}Aib_2His)$. Oxidation of decomposition products resulting in recoveries of the original peptide in excess of 50% have been observed for other copper(III)−peptide systems.[8]

Other products separated by HPLC were identified from NMR and mass spectra of HPLC fractions of products. The initial oxidized peptide product of the decomposition of $Cu^{III}(H_{-2}Aib_2His)$ was identified as α-aminoisobutyryl-α-aminoisobutyryl-α-hydroxyhistamine (Aib_2-α-OH-Ha), which dehydrates upon standing (when complexed to Cu(II)), to give α-aminoisobutyryl-α-aminoisobutyryl-α,β-dehydrohistamine (Aib_2-α,β-dehydro-Ha). The uncomplexed products are shown in Figure 8. The *cis*-isomer is shown for the olefin because this isomer was found in the crystal structure of the Cu(II) complex after the decomposition of Gly_2His.[12] Aib_2-α-OH-Ha was identified from a ^1H NMR spectrum of a product isolated by HPLC. A doublet of quartets at 3.05 ppm and a triplet at 5.57 ppm, which correspond to the α- and β-protons on the third residue of Aib_2-α-OH-Ha, respectively, was observed. Aib_2-α,β-dehydro-Ha was also identified from a ^1H NMR spectrum of a product isolated by HPLC. Doublets at 5.81 and 6.72 ppm, which correspond to the olefinic protons on the third residue, were observed. The mass spectrum of this product has a parent ion at 280 m/z, which corresponds to the $m + 1$ ion of Aib_2-α,β-dehydro-Ha. The overall reaction for

Table 6. NMR Data for Products

	chemical shifts		
	^1H, ppm		^{13}C, ppm
products	α	β	α-C
Aib_2-α-OH-Ha[a]	2.92 (d of q)	5.46 (t)	
Aib_2-α,β-dehydro-Ha[a]	5.70 (d)	6.61 (d)	
Gly_2-α-OH-Ha[b]	3.13 (m)	5.42 (m)	75.2
Gly_2-α,β-dehydro-H[b]	5.94 (d)	6.94 (d)	

[a] Varian VXR 500 MHz instrument. [b] Varian Gemini 200 MHz instrument.

the decomposition of $Cu^{III}(H_{-2}Aib_2His)$ in acid is shown in eq 24. The initial product, Aib_2-α-OH-Ha, is relatively stable in

$$2Cu^{III}(Aib_2His) + H_2O \rightarrow 2Cu^{II} + Aib_2His + Aib_2\text{-}\alpha\text{-}OH\text{-}Ha + CO_2 \quad (24)$$

acid, but its Cu(II) complex undergoes dehydration to produce the olefin.

Gly_2-α-OH-Ha and Gly_2-α,β-dehydro-Ha were observed as decomposition products of $Cu^{III}(H_{-2}Gly_2His)$. The identity of Gly_2-α-OH-Ha was confirmed by ^1H NMR and ^{13}C NMR. The ^1H NMR spectrum of Gly_2-α-OH-Ha is similar to the spectrum of Aib_2-α-OH-Ha. The ^{13}C NMR spectrum showed a peak at 75.2 ppm, which is consistent with a hydroxy group attached to the α-carbon of the third residue. On the basis of ^1H NMR data, Sakarai and Nakahara[13] also proposed Gly_2-α-OH-Ha as a product of the reaction of $Ni^{II}(H_{-2}Gly_2His)^-$ with O_2. Evidence of the formation of the olefin from O_2 oxidation of $Cu^{II}(H_{-2}Gly_2His)^-$ came from de Meester and Hodgson,[12] who reported the crystal structure of (glycylglycyl-α,β-dehydrohistidinato)copper(II). Our NMR data are summarized in Table 6 for oxidation products for both the $Cu^{III}(H_{-2}Aib_2His)$ and $Cu^{III}(H_{-2}Gly_2His)$ systems.

Reaction Mechanisms. Scheme 3 shows a possible mechanism for the decarboxylation of histidine-containing copper(III) tripeptide complexes where a second Cu(III) peptide provides an overall two electron oxidation to produce the oxidized peptide, a copper(II)−peptide, and CO_2. The rapid decarboxylation reaction resembles a pseudo-Kolbe electrolysis, the name given to anodic decarboxylations where electron transfer does not occur directly from the carboxylate group, but rather from a group attached to it.[21] $Cu^{III}(H_{-2}Aib_2His)$ and the corresponding complexes of Gly_2His and Ala_2His can be considered as pseudo-Kolbe species where Cu(III) is an electron-pair acceptor (remote from the carboxylate group) that permits the loss of CO_2. Scheme 3 shows Cu(III) reduction to a Cu(I)−DHP complex (as in Scheme 2) that would be a reactive intermediate quickly oxidized by a second Cu(III) and rapidly hydrolyzed to give the observed α-OH product.

An alternative mechanism (not shown) would be loss of CO_2 with formation of a Cu(II)-α-CH• intermediate that rapidly reacts with a second Cu(III) and with H_2O to produce the same product. These mechanisms (Cu(I) vs a Cu(II) carbon radical) cannot be distinguished from one another.

Conversion of Aib_2-α-OH-Ha to the olefin by dehydration was observed by chromatography and UV−vis spectroscopy. When the Cu(II)−peptide products were acidified immediately after loss of Cu(III), a chromatographic separation at pH 3.1 gave elution peaks for Aib_2His and Aib_2-α-OH-Ha but not for the olefin. If the decomposition solutions were held for 45 min at p[H+] 5.61 before acidification, the chromatographic peak

(21) Schafer, H. J. In *Topics in Current Chemistry*, Steckhan, E., Ed.; Springer-Verlag: Berlin, 1990, Vol. 152, pp 91−150.

Scheme 3. Proposed Mechanism for the Oxidative Decarboxylation of Histidine-Containing Cu(III) Tripeptides

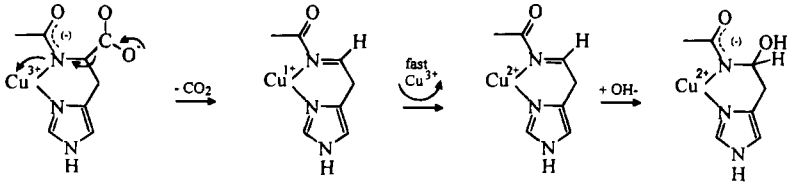

Scheme 4. Proposed Mechanism for the Decomposition of Histamine-Containing Cu(III) Tripeptides by Proton Abstraction

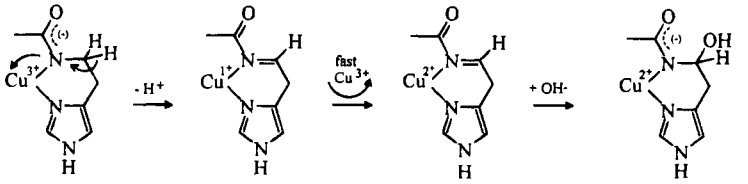

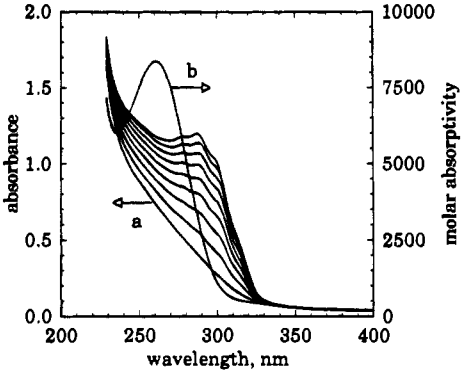

Figure 9. (a) Repetitive UV−vis scans for the formation of $Cu^{II}(Aib_2$-α,β-dehydro-Ha). Conditions: scan speed = 240 nm/min, cycle time = 170 s, path length = 1.0 cm, $[Cu^{II}(H_{-2}Aib_2$-α-OH-Ha)]$_{init} \sim 1.25 \times 10^{-4}$ M, p[H^+] 6.31. (b) UV−vis spectrum of the products formed after acidification to p[H^+] 1.8 to remove Cu(II).

for Aib_2-α-OH-Ha decreased and a peak due to Aib_2-α,β-dehydro-Ha was observed. Figure 9a shows the UV spectral changes over a period of 24 min for a $Cu^{II}(H_{-2}Aib_2$-α-OH-Ha) solution at p[H^+] 6.28 as the olefin forms. This reaction was also studied at 288 nm for 5700 s and gave excellent first-order kinetics with an observed rate constant of 5.9×10^{-4} s^{-1} at 25.0 °C, p[H^+] 6.28, and 0.50 M total phosphate buffer. The reaction was slower at p[H^+] 7.57 ($k_{obsd} = 6 \times 10^{-5}$ s^{-1}) and was also slower at p[H^+] 4.25 (where no reaction was seen after 5 min). Copper(II) is no longer complexed at low pH values. Figure 9b gives the spectrum of the olefin prepared from Cu(III) decomposition products that underwent dehydration at p[H^+] 6.28 and were then acidified to p[H^+] 1.8. The olefin has an intense absorption band at 261 nm ($\epsilon = 8370$ M^{-1} cm^{-1}) that corresponds to a $\pi-\pi^*$ transition and is well separated from other peptide absorbance peaks. The observed spectral characteristics are consistent with the identity of Aib_2-α,β-dehydro-Ha confirmed by ^1H NMR and mass spectrometry data.

Decomposition Products of $Cu^{III}(H_{-2}Aib_2Ha)^+$ and $Cu^{III}(H_{-2}Gly_2Ha)^+$. The copper(III) histamine-containing tripeptides are unable to undergo decarboxylation; however, the same decomposition products observed by HPLC for $Cu^{III}(H_{-2}Aib_2Ha)^+$ and $Cu^{III}(H_{-2}Gly_2Ha)^+$ were also observed for $Cu^{III}(H_{-2}Aib_2His)$ and $Cu^{III}(H_{-2}Gly_2His)$, respectively.

The decomposition of the copper(III) histamine-containing tripeptides occurs by proton abstraction from the α-carbon on the histamine residue to give the same products as does decarboxylation of the copper(III) histidine-containing tripeptides. Previous work has shown that the α-protons are ionizable and that abstraction of these protons leads to loss of copper(III).[8] Our work also shows that the abstraction of protons on the α-carbon are general-base catalyzed. Scheme 4 gives a possible mechanism for decomposition of the histamine complex to produce the observed products.

Conclusions

The reactivity of the copper(III) histidine-containing tripeptides toward self-decomposition increases in the order: $Cu^{III}(H_{-2}Aib_2His) < Cu^{III}(H_{-2}Ala_2His) < Cu^{III}(H_{-2}Gly_2His)$, where the increase in reactivity parallels an increase in reduction potentials. These decomposition reactions occur by oxidative decarboxylation with rate constants (k_d) that are 10^5-10^6 times larger than the decomposition of the corresponding histamine complexes. At physiological p[H^+] the reactivity of the histidine-containing compounds is greatest, whereas the reactivity of the histamine-containing tripeptides presented in this work and other tri- and tetrapeptides studied previously[8] is less. The pK_a for amine deprotonation of the histidine and histamine containing tripeptides are 2−3 pK_a units lower than those for other peptides.

Acknowledgment. This work was supported by Public Health Service Grant No. GM 12152 from the National Institute of General Medical Sciences and by National Science Foundation Grant CHE-9024291.

IC9405687